

Modification of auxinic phenoxyalkanoic acid herbicides by the acyl acid amido synthetase GH3.15 from *Arabidopsis*

Ashley M. Sherp, Soon Goo Lee, Evelyn Schraft, Joseph M. Jez*

Department of Biology, Washington University, St. Louis, MO 63130, USA

**Corresponding author; E-mail: jjez@wustl.edu*

Running title: Herbicide modification by an acyl acid amido synthetase

Keywords: *Arabidopsis thaliana*, auxin, enzyme kinetics, herbicides, x-ray crystallography, Gretchen Hagen 3, herbicide tolerance, acyl acid amido synthetase, 2,4-D, structure-activity relationship

Herbicide-resistance traits are the most widely used agriculture biotechnology products. Yet, to maintain their effectiveness and to mitigate selection of herbicide-resistant weeds, the discovery of new resistance traits that use different chemical modes of action is essential. In plants, the Gretchen Hagen 3 (GH3) acyl acid amido synthetases catalyze the conjugation of amino acids to jasmonate and auxin phytohormones. This reaction chemistry has not been explored as a possible approach for herbicide modification and inactivation. Here, we examined a set of *Arabidopsis* GH3 proteins that use the auxins indole-3-acetic acid (IAA) and indole-3-butyric acid (IBA) as substrates along with the corresponding auxinic phenoxyalkanoic acid herbicides 2,4-dichlorophenoxyacetic acid (2,4-D) and 4-(2,4-dichlorophenoxy)butyric acid (2,4-DB). The IBA-specific AtGH3.15 protein displayed high catalytic activity with 2,4-DB, which was comparable to its activity with IBA. Screening of phenoxyalkanoic and phenylalkyl acids indicated that side-chain length of alkanolic and alkyl acids is a key feature of AtGH3.15's substrate preference. The X-ray crystal structure of the AtGH3.15•2,4-DB complex revealed how the herbicide binds in the active site. In root elongation assays, *Arabidopsis* AtGH3.15-knockout and -overexpression lines grown in the presence of 2,4-DB exhibited

hypersensitivity and tolerance, respectively, indicating that the AtGH3.15-catalyzed modification inactivates 2,4-DB. These findings suggest a potential use for AtGH3.15, and perhaps other GH3 proteins, as herbicide-modifying enzymes that employ a mode of action different from those of currently available herbicide resistance traits.

Herbicide-resistance traits accounted for 47% of genetically-engineered soybean, maize, canola, cotton, sugar beet, and alfalfa plantings worldwide in 2017 (1). Since the introduction of the first crops with a glyphosate-resistant trait, the use of herbicides with distinct modes of action and the discovery of new resistance traits have become critical elements for increased agricultural productivity and for effective management of weed resistance (2-3). For example, auxinic herbicides, based on phenoxyalkanoic acid, benzoic acid, pyridine carboxylic acid, and quinoline carboxylic acid chemical scaffolds mimic the plant hormone auxin (indole-3-acetic acid; IAA) and are used extensively in agronomic and non-crop applications for broadleaf weed control (Fig. 1) (4-5). These molecules elicit the same type of growth and developmental responses as IAA, but due to higher stability in the plant result in longer-lasting and stronger effects such as plant overgrowth (4-5).

Of the auxinic herbicides, 2,4-dichlorophenoxyacetic acid (2,4-D; Fig. 1)

was the first to be commercialized in 1945 and is the most widely used phenoxyalkanoic acid herbicide with ~46 million pounds applied in the US per year, predominantly in the Midwest, Great Plains, and the Northwestern United States (6-7). Related to 2,4-D, 4-(2,4-dichlorophenoxy)butyric acid (2,4-DB; **Fig. 1**) has also been used to control annual and perennial broadleaf weeds since 1958 (8-9). After foliar application, 2,4-DB is taken up by the leaves and roots and converted through peroxisomal β -oxidation to the active herbicide 2,4-D (8-10). At the molecular level, 2,4-D binds to the auxin receptor F-box protein TIR1, which facilitates interaction between the receptor and co-repressor Aux/IAA proteins (11-12). This leads to ubiquitination and degradation of the Aux/IAA proteins to modulate downstream interactions with auxin response factors that control transcription of auxin responsive genes (13-14). Although both IAA and 2,4-D target the auxin receptor, 2,4-D is metabolized more slowly than IAA, which enhances herbicidal effects through elevated expression of auxin responsive genes leading to plant death (6, 15-16). For agricultural biotechnology applications, herbicide tolerance traits have relied on the identification of enzymes that either chemically inactivate the herbicide or prevent inhibition of a target by the herbicide (17-24). For example, isolation of a microbial aryloxyalkanoate dioxygenase that cleaves 2,4-D provides tolerance to this auxinic herbicide and is the basis for 2,4-D resistant crops currently entering the market (23). Access to tolerance traits with distinct modes of action is critical for reducing the emergence of herbicide resistant weeds (2-6).

In plants, the Gretchen Hagen 3 (GH3) acyl acid amido synthetases conjugate amino acids to carboxylic acid-containing hormones, such as jasmonic acid, IAA, and

the endogenous auxin indole-3-butyric acid (IBA), to regulate plant growth, seed development, light signaling, and pathogen responses (25-33). GH3 proteins catalyze the adenylation of the carboxylate on these molecules to form an acyl-AMP intermediate, which undergoes nucleophilic attack by an amino acid to yield the conjugated product (28, 30). Biochemical and structural studies of GH3 proteins from *Arabidopsis thaliana* have identified jasmonate-, IAA-, and IBA-specific members of the family (25-27, 29, 32-33).

Given the chemical similarity between phenoxyalkanoic acids (i.e., 2,4-D and 2,4-DB) and auxins (IAA and IBA) (**Fig. 1**), we examined the potential of selected *Arabidopsis* GH3 proteins to modify either 2,4-D or 2,4-DB. The IBA-specific *Arabidopsis* GH3.15 protein (AtGH3.15) displayed high catalytic activity with 2,4-DB, which was comparable to that of IBA, and the X-ray crystal structure of the enzyme in complex with the herbicide shows how the molecule binds in the active site. When grown on 2,4-DB, *A. thaliana* T-DNA insertions in *AtGH3.15* and 35S:FLAG-AtGH3.15 overexpression lines show hypersensitivity and tolerance, respectively, in root elongation assays. These findings suggest a potential use for AtGH3.15, and perhaps other GH3 proteins, as herbicide-modifying enzymes that employ a mode of action that differs from available auxinic herbicide resistance traits.

RESULTS

Screen of *Arabidopsis* GH3 proteins with 2,4-D and 2,4-DB and comparison to auxin substrates. The auxinic herbicides 2,4-D and 2,4-DB mimic the biological activity of the endogenous auxins IAA and IBA, respectively. Previous biochemical studies identified IAA- and IBA-specific GH3 acyl acid amido synthetases from *Arabidopsis* (26, 32-33). Using purified

recombinant protein, we examined the ability of the IAA-modifying AtGH3.1, AtGH3.2, AtGH3.5, and AtGH3.17 (32) and the IBA-modifying AtGH3.15 (33) to use either 2,4-D or 2,4-DB as substrates (**Table 1; Fig. 2**). None of the IAA-specific Arabidopsis GH3 proteins tested used 2,4-D as a substrate; however, AtGH3.15 exhibited a low activity with this herbicide. Except for AtGH3.1, the GH3 proteins accepted 2,4-DB as a substrate to varying degrees. The most efficient enzyme was the IBA-specific AtGH3.15 with a catalytic efficiency (k_{cat}/K_m) 3- to 5-fold higher than AtGH3.2 and AtGH3.5, respectively. AtGH3.17 had the lowest activity, roughly 50-fold that of AtGH3.15, with 2,4-DB as a substrate. For comparison, previously reported data on these GH3 proteins (32-33) with the auxin substrates IAA and IBA are summarized (**Table 1; Fig. 2**). Although 2,4-D mimics the biological effect of IAA, it is not used as a substrate for the four IAA-modifying GH3 proteins examined here and is a poor substrate for the IBA-specific AtGH3.15. In contrast to the 2,4-D/IAA pairing, the catalytic efficiencies of AtGH3.2, AtGH3.5, AtGH3.15, and AtGH3.17 for the 2,4-DB/IBA pair were generally comparable with AtGH3.15 as the most robust enzyme for these molecules.

Biochemical analysis of AtGH3.15. As the most active GH3 protein tested with 2,4-DB, AtGH3.15 was further characterized for its amino acid substrate profile and with other phenoxyalkanoic and phenylalkyl acids. As noted above, biochemical analysis of AtGH3.15 yielded steady-state kinetic parameters for 2,4-DB that were comparable to those obtained for IBA with glutamine (**Table 1**). QTRAP mass spectrometry analysis confirmed formation of the 2,4-DB-glutamine conjugate in vitro. Incubation of AtGH3.15 with 2,4-DB, ATP, and glutamine lead to formation of the conjugate

(deprotonated molecular ion (M-H)⁻ m/z = 376.2; **Fig. S1**). Assays in the absence of protein or any one substrate did not yield a peak corresponding to the conjugated product. To confirm that the amino acid preference of AtGH3.15 was the same with 2,4-DB as with IBA, the substrate profile was examined using 2,4-DB and each amino acid (**Fig. S2**). The amino acid profile was the same for AtGH3.15 with 2,4-DB as with IBA (33) with cysteine, histidine, methionine, glutamine, and tyrosine having the highest activity. Steady-state kinetics with cysteine, histidine, methionine, glutamine, and tyrosine were determined and confirm that, as with IBA, glutamine is the preferred amino acid for AtGH3.15 with 2,4-DB (**Table 2**).

To determine if AtGH3.15 was active with other auxinic herbicides (**Fig. S3**), the benzoic acid dicamba (3,6-dichloro-2-methoxybenzoic acid), the pyridine carboxylic acids clopyralid (3,6-dichloropyridine-2-carboxylic acid), picloram (4-amino-3,5,6-trichloro-2-pyridine carboxylic acid), and triclopyr ([3,5,6-trichloro-2-pyridinyl]oxy]acetic acid), and the phenoxyalkanoic acids dichlorprop (2-(2,4-dichlorophenoxy)propanoic acid), mecoprop (2-(4-chloro-2-methylphenoxy)propionic acid), 4-chloro-2-methylphenoxy acetic acid (MCPA), 2,4,5-trichlorophenoxyacetic acid (2,4,5-T), and 4-(4-chloro-2-methylphenoxy)butanoic acid (MCPB) were tested as substrates. AtGH3.15 displayed no detectable activity with dicamba, the pyridine carboxylic acids, dichlorprop, mecoprop, and MCPA. The catalytic efficiency of AtGH3.15 with 2,4,5-T was comparable to that with 2,4-D (**Table 3**). Similarly, AtGH3.15 accepted MCPB as a substrate with a k_{cat}/K_m 1.8-fold lower than either 2,4-DB or IBA (**Table 3**). Chemically, MCPB is identical to 2,4-DB except for a methyl group substituted for a

chlorine at C2 (**Fig. S3**). These results are consistent with a preference for longer-chain phenoxyalkanoic acids.

To further probe the structure-activity relationship of AtGH3.15 assays were performed with phenoxybutanoic and phenylalkyl acids (**Fig. S3; Table 3**). Kinetic analysis with 4-(2-chlorophenoxy)butanoic acid and 4-(2,6-dimethylphenoxy)butanoic acid suggests that the removal of the chlorine from the C4 position does not reduce catalytic efficiency; however, extension of this position reduces catalytic activity, as observed with 4-(4-methoxyphenoxy)butanoic acid. Comparison of the catalytic efficiencies of 4-phenoxybutyric acid, 4-phenylbutyric acid, 5-phenylvaleric acid, and 5-(4-fluorophenyl)valeric acid also indicate that compounds longer in length from carboxylate to the substituted phenyl group are superior substrates.

Three-dimensional structure of AtGH3.15 in complex with 2,4-DB. To provide insight on how 2,4-DB interacts with AtGH3.15, the protein was crystallized in the presence of the ligand. The 2.15 Å resolution structure of the AtGH3.15•2,4-DB complex was solved by molecular replacement (**Table 4; Fig. 3A**). The overall fold of the resulting structure was similar (1.4 Å² root mean square deviation for 550 C_v-atoms) to that of the previously reported AtGH3.15•AMP complex (33) with the conformationally mobile C-terminal domain adopting the 'open' active site conformation. Examination of the electron density maps in the active site revealed two large patterns of density in the acyl acid binding site, which were subsequently modeled and refined as two molecules of 2,4-DB (**Fig. 3B**). Comparison with the position of AMP in the AtGH3.15•AMP complex indicates that only one 2,4-DB molecule is positioned in an orientation that

points the reactive carboxylate group toward the phosphate group that undergoes the adenylation reaction (**Fig. 3C**). This 2,4-DB molecule stacks with Phe166, forms a hydrogen bond contact with Ser122 (which was modeled in two alternate side-chain conformations), and is situated in a space bordered by Met162, Val163, Phe325, and Phe332 (**Fig. 3D**). The second 2,4-DB molecule positions its carboxylate group away from the nucleotide binding site and is situated deeper in the acyl acid binding site (**Fig. 3C**). This ligand forms a charge-charge interaction between its carboxylate and the side-chain of Arg214 (**Fig. 3D**). Ser299 contributes a hydrogen bond interaction to the carboxylate. The substituted phenyl ring is positioned to form van der Waals contacts with Ile143, Leu181, and Phe219. It is not clear if the binding of two 2,4-DB molecules in the acyl acid site of AtGH3.15 is biochemically relevant or is an artifact of crystallization. Because of the large size of the site, it is possible that binding of one ligand deeper in the pocket positions the second for efficient catalysis.

Effect of AtGH3.15 knockout and overexpression in Arabidopsis on 2,4-DB and 2,4-D treatment. 2,4-DB, like IBA, inhibits primary root elongation (34-36). To determine if the *in vitro* activity of AtGH3.15 with 2,4-DB had *in planta* effects, previously generated and characterized knockout and overexpression lines of AtGH3.15 (33) were used in primary root elongation assays with 2,4-DB. Seedlings of wild-type, two T-DNA insertion lines (SALK_108265 and SALK_079153), and three overexpression lines (35S:FLAG-GH3.15 1-5, 35S:FLAG-GH3.15 2-7, and 35S:FLAG-GH3.15 8-2) were grown on 1 μM 2,4-DB for 10 days to determine if altered expression of AtGH3.15 altered plant responses to 2,4-DB treatment (**Fig. 4**). Mock-treated seedlings were

comparable between the various lines (**Fig. 4A**, upper panels). Seedlings treated with 1 μ M 2,4-DB (**Fig. 4A**, lower panels) showed statistically significant differences between wild-type Col-0, SALK_108265, SALK_079153, 35S:FLAG-GH3.15 1-5, 35S:FLAG-GH3.15 2-7, and 35S:FLAG-GH3.15 8-2 (**Fig. 4B**). The T-DNA knockout lines (SALK_108265 and SALK_079153) showed hypersensitivity to treatment with 2,4-DB compared to wild-type Col-0 (**Fig. 4**). The overexpression lines (35S:FLAG-GH3.15 1-5, 35S:FLAG-GH3.15 2-7, and 35S:FLAG-GH3.15 8-2) were resistant to treatment with 2,4-DB compared to wild-type Col-0, as they maintained active root elongation in the presence of the herbicide (**Fig. 4**). As AtGH3.15 uses IBA and 2,4-DB, but does not prefer either IAA or 2,4-D as a substrate *in vitro*, wild-type Col-0, knockout, and overexpression lines were also screened on 2,4-D in the root elongation assay. There were no statistically significant differences between wild-type, T-DNA insertion, and overexpression lines grown on 20 nM, 40 nM, or 80 nM 2,4-D for 10 days (**Fig. S4**), which is consistent with AtGH3.15 either not having a role in 2,4-D metabolism or downstream herbicide effects.

DISCUSSION

Multiple studies highlight the diverse roles for GH3 acyl acid amido synthetases as modulators of jasmonate and auxin phytohormones (25-33), but the potential function of these proteins as modifiers of herbicides in plants has not been fully examined. Motivated by the possibility that the phenoxyalkanoic acid auxinic herbicides 2,4-D and 2,4-DB mimic IAA and IBA (**Fig. 1**), respectively, in triggering auxin-linked responses, we examined if GH3 proteins that conjugate amino acids to these hormones can modify 2,4-D and 2,4-DB. Surprisingly, the IAA-modifying GH3 proteins (AtGH3.1,

AtGH3.2, AtGH3.5, and AtGH3.17) did not have activity with 2,4-D (**Table 1; Fig 2**). This suggests that although 2,4-D is a potent IAA analog targeting the TIR1 auxin receptor, it does not serve as an IAA mimic for the GH3 proteins. This difference may contribute to potentiation of the herbicidal effect of 2,4-D.

In contrast, AtGH3.15 is highly active with both IBA and its auxinic herbicide counterpart 2,4-DB (**Table 1; Fig 2**). Additional biochemical analysis with a range of substrates (**Fig. S3**) shows that AtGH3.15 does not accept benzoic acid (dicamba), pyridine carboxylic acid (clopyralid, picloram, and triclopyr), and short side-chain phenoxyalkanoic acid (dichlorprop, mecoprop, MCPA) auxin herbicides as substrates. AtGH3.15 did use of 2,4-D and 2,4,5-T, which differs from 2,4-D by one additional chlorine, but with catalytic efficiencies 50- to 100-fold lower than that observed with either IBA or 2,4-DB (**Tables 1 & 3; Fig 2**). The kinetic analysis with MCPB, an analog of 2,4-DB, and other longer side-chain phenoxyalkanoic acid and phenylalkyl acid substrates indicates that substitutions of the phenyl group are not as important as side-chain length for activity; however, changes to phenyl group substituents that lengthen the moieties, such as the methoxy group of 4-(4-methoxyphenoxy)butanoic acid, reduce catalytic efficiency (**Table 3**).

The x-ray crystal structure of AtGH3.15 in complex with 2,4-DB (**Fig. 3**) provides insight on how this molecule is recognized largely through apolar surface contacts, although some hydrogen bond interactions contribute. The orientation of one 2,4-DB molecule in the active site with its reactive carboxylate toward the location of the ATP/AMP binding site suggests how a productive first-half reaction leading to the adenylated reaction intermediate occurs. As noted in the results, the binding of two 2,4-

DB molecules in the acyl acid site of AtGH3.15 maybe biochemically relevant or an artifact of crystallization, but is not unprecedented. For example, a set of stacked alrestatin molecules in aldose reductase was proposed to contribute to ligand specificity (34). It is possible that the large size of the AtGH3.15 acyl acid binding site and binding of two substrates in different orientations contributes to efficient catalysis. This detail requires additional detailed biochemical analyses. Overall, the AtGH3.15•2,4-DB complex is the first of a GH3 protein with a herbicide bound and shows how binding in the site is largely dictated by surface contacts.

The *in planta* effect of AtGH3.15 knockout or overexpression indicates that changes in expression alter sensitivity to 2,4-DB (**Fig. 4**). Previous work characterized these plant lines (33). In the root elongation assays with Arabidopsis seedlings (**Fig. 4**), knockout lines of AtGH3.15 showed hypersensitivity to treatment with 2,4-DB, whereas, overexpression lines of AtGH3.15 displayed clear tolerance to 2,4-DB. As with other plants, metabolism of 2,4-DB to 2,4-D by β -oxidation in the peroxisome, a process similar to conversion of IBA to IAA, leads to auxinic herbicide effects in Arabidopsis (35-37). Interestingly, this experiment with AtGH3.15 and 2,4-DB, along with other reported studies of various GH3 proteins and their responses to different phytohormones such as IAA, IBA, and jasmonates (25-26, 30, 32-33), highlight differences between *in vitro* steady-state kinetics and *in planta* responses. The K_m values reported for various GH3 proteins with their cognate plant hormone substrates are typically in the 300-800 μM range; however, overexpression and knockout plant lines of the different GH3-encoding genes exhibit growth phenotypes with phytohormone treatments in the range of 1-10 μM that

correspond to GH3 protein expression changes (25-26, 30, 32-33). These differences highlight the need for further investigations into the metabolism of these molecules, which may alter local concentrations within different tissues and cell types of the plant and the fluxes that control plant growth and development.

Overall, the biochemical and *in planta* analysis of AtGH3.15 suggests a possible model for how altered expression affects plant growth (**Fig. 5**). Loss of AtGH3.15 in the T-DNA insertion lines would remove background conjugation to 2,4-DB, allowing more of the herbicide to be metabolized in the peroxisome (35-37). This results in the shortened root phenotype compared to wild-type Arabidopsis seedlings. In contrast, overexpression of AtGH3.15 would increase 2,4-DB conjugate formation, which results in the observed tolerance to herbicide treatment and the longer root phenotype. This parallels the effect of treating Arabidopsis AtGH3.15 knockout and overexpression lines with the auxin IBA (33). Overall, the biochemical, structure, and *in planta* experiments suggest the use of AtGH3.15 as a possible resistance trait for 2,4-DB.

While monocots and leguminous plants are inherently tolerant to 2,4-DB application, they are not completely resistant and dicots remain susceptible (4-9). Overexpression of AtGH3.15 *in planta* could potentially enhance the tolerance of plants to 2,4-DB application. There are several possible advantages to exploring AtGH3.15 as a possible 2,4-DB resistance trait. In comparison to overexpression of IAA-specific GH3 proteins, which results in severe growth phenotypes, such as dwarfing (29), overexpression of AtGH3.15 in Arabidopsis yielded no detrimental growth changes (33). Moreover, the distinct amino acid substrate profile of AtGH3.15 versus the IAA-specific proteins (**Table 2; Fig S2**),

which primarily use aspartate and glutamate, may help maintain inactive forms of 2,4-DB and contribute to tolerance (25-33). Amino acid conjugated forms of IAA have varied roles with the IAA-aspartate and IAA-glutamate conjugates leading to hormone degradation and IAA-alanine and IAA-leucine conjugates providing storage forms of the auxin (31, 38-39). The best-studied IAA and 2,4-D conjugates are those of aspartate and glutamate, which suggests that these molecules can be hydrolyzed back into free acid forms (39). With 2,4-D conjugates this contributes to maintaining the effect of the herbicide (39). Currently, there is a lack of information on the metabolic fates of IBA and auxinic herbicides conjugated to other amino acids. Potential glutamine, cysteine, histidine, methionine, and tyrosine conjugates of IBA and 2,4-DB formed by AtGH3.15 need to be more fully explored with regard to biological fate and herbicide action.

In addition to the activity of AtGH3.15 with 2,4-DB, the structure of this enzyme in complex with the herbicide serves as a starting point to engineer variants that modify 2,4-D with amino acids that are neither aspartate nor glutamate, as a means of exploiting potential differences in herbicide metabolism. As 2,4-D is a widely used herbicide, the ability to engineer activity of AtGH3.15 with 2,4-D would result in a greater agricultural impact than with 2,4-DB. Before the discovery and commercialization of auxin herbicides, like 2,4-D, perennial weeds were particularly difficult to control (40); however, to reduce the development of weeds with herbicide resistance multiple different modes of action for tolerance traits are needed. For example, extensive reliance on glyphosate in early agricultural biotech crops led to selection of weed populations with inherent tolerance to the herbicide and spurred the development of new herbicide resistance traits.

To date, the molecular basis for enzyme-based herbicide protection strategies rely on a limited number of mechanisms - the use of modified enolpyruvylshikimate-3-phosphate synthase to prevent inhibition by glyphosate and glufosinate (21); acetylation of herbicide (18-19); degradation of 2,4-D by aryloxyalkanoate dioxygenases (23); conversion of dicamba by mono-oxygenases (22); modification of acetolactate synthase to prevent inhibition by sulfonylurea herbicides; degradation of oxynil herbicide by a nitrilase (24); and use of *p*-hydroxyphenylpyruvate dioxygenases for mesotrione and isoxaflutole tolerance (20). Amino acid conjugation of herbicides may provide an additional resistance mechanism.

The benefits of herbicide-tolerant crops and the selection of resistant weeds, highlights the importance of discovery and development of new modes-of-action for herbicide tolerance. Stacked traits, the ability to tolerate different herbicidal applications, are also important for the future of herbicide tolerance in genetically modified crops to help combat the selection of herbicide resistant weeds in the future (41). The development of 2,4-DB tolerant crops via expression of AtGH3.15, or the use of an engineered variant that efficiently conjugates 2,4-D, would help to broaden the tool kit of herbicidal tolerance modes of action.

EXPERIMENTAL PROCEDURES

Protein preparation, enzymatic analyses, and site-directed mutagenesis.

Recombinant AtGH3.1, AtGH3.2, AtGH3.5, AtGH3.15, and AtGH3.17 were expressed in *E. coli* and purified by nickel-affinity and size-exclusion chromatographies (32-33). Enzymatic activity of various GH3 proteins was monitored using a coupled-enzyme assay system (28, 32-33). Standard conditions were 50 mM Tris (pH 8.0), 3 mM MgCl₂, 1 mM ATP, 1 mM

phosphoenolpyruvate, 0.2 mM NADH, 2 units myokinase, 4 units pyruvate kinase, 4 units lactate dehydrogenase and 10 μ g protein in a 200 μ L reaction volume. Concentrations used for various assays are noted in table legends. Reactions were performed in a 96-well plate format with initial velocity data acquired on a Tecan Infinite 200 with data fit to the Michaelis-Menten equation using SigmaPlot.

Mass spectrometry. Reactions were performed in the presence and absence of ~20 μ g AtGH3.15 with 50 mM Tris (pH 8), 3 mM MgCl₂, 2 mM ATP, 2 mM 2,4-DB, and 2 mM glutamine in a 200 μ l volume. Reactions were allowed to react for 10 minutes at room temperature and then placed at -20 °C. The reactions were directly infused into the mass spectrometer. The MS1 (Q1) scan was acquired with the 6500-QTRAP (Sciex) in low mass (LM) electrospray ionization in negative ion mode at a capillary voltage of -4500 and a mass range of 50-600 m/z .

Protein crystallography. Crystals of AtGH3.15 in complex with 2,4-DB were grown by vapor diffusion in hanging drops of a 1:1 mixture of protein (13 mg mL⁻¹) and crystallization buffer (1.2 M potassium phosphate (dibasic)/0.8 M sodium phosphate (monobasic) and 0.1 M sodium acetate/acetic acid, pH 4.5) with 2.5 mM 2,4-DB at 4 °C. Crystals were frozen in liquid nitrogen with mother liquor supplemented with 15% (v/v) glycerol as a cryoprotectant. Diffraction data was collected at the SBC-19ID beamline of the Argonne National Laboratory Advanced Photon Source (APS) with indexing and scaling performed using HKL3000 (42). Molecular replacement was performed using PHENIX (43) with the three-dimensional structure of AtGH3.15 (PDB: 6AVH; 33) as a search model. Model building and

refinement were performed with COOT (44) and PHENIX, respectively. Data collection and refinement statistics are summarized in **Table 4**. Coordinates and structure factors were deposited in the PDB (PDB: 6E1Q).

Arabidopsis knockout and overexpression lines and root elongation assays. Confirmation and characterization of the two homozygous T-DNA insertion lines (SALK_108265C and SALK_071953) in the At5g13370 gene that codes for AtGH3.15 was previously described (33). Generation and characterization of the three independent *A. thaliana* Col-0 lines overexpressing N-terminally FLAG-tagged AtGH3.15 under control of the cauliflower mosaic virus 35S promoter was also previously reported (33). Root elongation assays to examine the effect of AtGH3.15 expression changes on resistance to 2,4-D and 2,4-DB, used seeds that were surface sterilized with 70% (v/v) ethanol for 5 min, 90% (v/v) ethanol for 1 min, and resuspended in 0.1% (w/v) sterile agar. Sterilized seeds were stratified at 4 °C for 2-4 days and plated on Murashige and Skoog (MS) plates with 0.6% (w/v) agar and supplemented with 0.5% (v/v) sucrose. Treatments were performed at 1 μ M 2,4-DB and 20, 40 and 80 nM 2,4-D with mock-treated plates receiving equivalent amounts of 70% (v/v) ethanol (2,4-DB and 2,4-D were dissolved in 70% ethanol). Plates were sealed with 3M micropore tape and incubated at 22 °C under continuous white light for 10 days. Seedlings were excised from media and measured using a ruler. Percent root length versus mock-treated was calculated as: (root length of treated seedlings)/(average root length of mock treated seedlings)*100.

ACKNOWLEDGEMENTS

This work was supported by the NSF (MCB-1614539 to J.M.J.). A.M.S was an

NSF Graduate Research Fellow (DGE-1143954). The mass spectrometry measurement was performed at the Proteomics & Mass Spectrometry Facility at the Donald Danforth Plant Science Center based upon work supported by grants from the National Science Foundation (DBI-1427621) for acquisition of the 6500 QTRAP LC-MS/MS. Portions of this research were carried out at the Argonne National Laboratory Structural Biology Center of the Advanced Photon Source, a national use facility operated by the University of Chicago for the Department of Energy Office of Biological and Environmental Research under Grant DE-AC02-06CH11357.

CONFLICT OF INTEREST STATEMENT

The authors have no competing financial interests.

AUTHOR CONTRIBUTIONS

A.M.S. and J.M.J. designed the research; A.M.S., S.G.L., and E.S. performed the research; A.M.S., S.G.L., and J.M.J. analyzed data; A.M.S. and J.M.J. wrote the paper with all authors providing editorial input.

REFERENCES

1. ISAAA (2017) Global status of commercialized biotech/GM crops in 2017. *ISAAA Brief No. 53* (ISAAA, Ithaca, NY).
2. Shaner DL (2000) The impact of glyphosate-tolerant crops on the use of other herbicides and on resistance management. *Pest. Manag. Sci.* **56**, 320-326.
3. Service RF (2007) Agbiotech: a growing threat down on the farm. *Science* **316**, 1114-1117.
4. Grossmann K (2010) Auxin herbicides: current status of mechanism and mode of action. *Pest. Manag. Sci.* **66**, 113-120.
5. Song Y (2014) Insight into the mode of action of 2,4-dichlorophenoxyacetic acid (2,4-D) as an herbicide. *J. Int. Plant Biol.* **56**, 106-113.
6. Peterson MA, McMaster SA, Riechers DE, Skelton J, Stahlman PW (2016) 2,4-D past, present, and future: a review. *Weed Tech.* **30**, 303-345.
7. United States Environmental Protection Agency (2005) *Registration Eligibility Decision (RED) 2,4-D*, EPA-738-F-05-002.
8. Charles JM, Cifone MA, Lawlor T, Murli H, Young RR, Leeming NM (2000) Evaluation of the in vitro genetic toxicity of 4-(2,4-dichlorophenoxy) butyric acid. *Mutat. Res.* **472**, 75-83.
9. United States Environmental Protection Agency (2005) *Registration Eligibility Decision (RED) 2,4-DB*, EPA-738-F-05-001.
10. Rao VS (1940) Herbicide transformations in plants. *Principles of Weed Science* (Science Publishers, Enfield, NH), pp 199-231.
11. Dharmasiri N, Dharmasiri S, Estelle M (2005) The F-box protein TIR1 is an auxin receptor. *Nature* **435**, 441-445.
12. Kepinski S, Leyser O (2005) The *Arabidopsis* TIR1 protein is an auxin receptor. *Nature* **435**, 446-451.
13. Salehin M, Bagchi R, Estelle M (2015) SCFTIR1/AFB-based auxin perception: mechanism and role in plant growth and development. *Plant Cell* **27**, 9-19.
14. Korasick DA, Jez JM, Strader LC (2015) Refining the nuclear auxin response pathway through structural biology. *Curr. Opin. Plant Biol.* **27**, 22-28.
15. Enders TA, Strader LC (2015) Auxin activity: past, present, and future. *Amer. J. Bot.* **102**, 180-196.
16. Sterling TM, Hall JC (1997) Mechanism of action of natural auxins and the auxinic herbicides. *Toxicology, Biochemistry and Molecular Biology of Herbicide Activity*, eds Roe RM, Burton JD, Kuhr RJ (IOS Press, Amsterdam), pp 111-141.
17. Chaleff RS, Mauvais CJ (1984) Acetolactate synthase is the site of action of two sulfonylurea herbicides in higher plants. *Science* **224**, 1443-1445.
18. D'Halluin K, De Block M, Denecke J, Janssens J, Reynaerts A, Botterman J (1992) The bar gene as selectable and screenable marker in plant engineering. *Methods Enzymol.* **216**, 415-426.
19. Castle LA, Siehl DL, Gorton R, Patten PA, Chen YH, Bertain S, Cho HJ, Duck N, Wong J, Liu D, Lassner MW (2004) Discovery and directed evolution of a glyphosate tolerance gene. *Science* **304**, 1151-1154.
20. Rippert P, Scimemi C, Dubald M, Matringe M (2004) Engineering plant shikimate pathway for production of tocotrienol and improving herbicide resistance. *Plant Physiol.* **134**, 92-100.
21. Tan S, Evans R, Singh B (2006) Herbicidal inhibitors of amino acid biosynthesis and herbicide-tolerant crops. *Amino Acids* **30**, 195-204.

22. Behrens MR, Mutlu N, Chakraborty S, Dumitru R, Jiang WZ, Lavalley BJ, Herman PL, Clemente TE, Weeks DP (2007) Dicamba resistance: enlarging and preserving biotechnology-based weed management strategies. *Science* **316**, 1185-1188.
23. Wright TR, Shan G, Walsh TA, Lira JM, Cui C, Song P, Zhuang M, Arnold NL, Lin G, Yau K, Russell SM, Cicchillo RM, Peterson MA, Simpson DM, Zhou N, Ponsamuel J, Zhang Z (2010) Robust crop resistance to broadleaf and grass herbicides provided by aryloxyalkanoate dioxygenase transgenes. *Proc. Natl. Acad. Sci. USA* **107**, 20240-20245.
24. Detzel C, Maas R, Tubeleviciute A, Jose J (2013) Autodisplay of nitrilase from *Klebsiella pneumoniae* and whole-cell degradation of oxynil herbicides and related compounds. *Appl. Micro. Biotech.* **97**, 4887-4896.
25. Staswick PE, Tiraki I, Rowe ML (2002) Jasmonate response locuse JAR1 and several related Arabidopsis genes encode enzymes of the firefly luciferase superfamily that show activity on jasmonic, salicylic, and indole-3-acetic acids in an assay for adenylation. *Plant Cell* **14**, 1405-1415.
26. Staswick PE, Serban B, Rowe M, Tiryaki I, Maldonado MT, Maldonado MC, Suza W (2005) Characterization of an Arabidopsis enzyme family that conjugates amino acids to indole-3-acetic acid. *Plant Cell* **17**, 616-627.
27. Terol J, Domingo C, Talón M (2006) The GH3 family in plants: Genome wide analysis in rice and evolutionary history based on EST analysis. *Gene* **371**, 279-290.
28. Chen Q, Westfall CS, Hicks LM, Wang S, Jez JM (2010) Kinetic basis for the conjugation of auxin by a GH3 family indole acetic acid-amido synthetase. *J. Biol. Chem.* **285**, 29780-29786.
29. Westfall CS, Herrmann J, Chen Q, Wang S, Jez JM (2010) Modulating plant hormone levels by enzyme action: the GH3 family of acyl acid amido synthetases. *Plant Signal. Behav.* **5**, 1597-1602.
30. Westfall CS, Zubieta C, Herrmann J, Kapp U, Nanao MH, Jez JM (2012) Structural basis for pre-receptor modulation of plant hormones by GH3 family proteins. *Science* **336**, 1708-1711.
31. Westfall CS, Muehler AM, Jez JM (2013) Enzyme action in the regulation of plant hormone responses. *J. Biol. Chem.* **288**, 19304-19311.
32. Westfall CS, Sherp AM, Zubieta C, Alvarez S, Schraft E, Marcellin R, Ramirez L, Jez JM (2016) *Arabidopsis thaliana* GH3.5 acyl acid amido synthetase mediates metabolic crosstalk in auxin and salicylic acid homeostasis. *Proc. Natl. Acad. Sci. USA* **113**, 13917-13922.
33. Sherp AM, Westfall CS, Alvarez S, Jez JM (2018) *Arabidopsis thaliana* GH3.15 acyl acid amido synthetase has a highly specific substrate preference for the auxin precursor indole-3-butyric acid. *J. Biol. Chem.* **293**, 4277-4288.
34. Harrison DH, Bohren KM, Petsko GA, Ringe D, Gabbay KH (1997) The alrestatin double-decker: binding of two inhibitor molecules to human aldose reductase reveals a new specificity determinant. *Biochemistry* **36**, 16134-16140.
35. Zolman BK, Yoder A, Bartel B (2000) Genetic analysis of indole-3-butyric acid responses in *Arabidopsis thaliana* reveals four mutant classes. *Genetics* **156**, 1323-1337.
36. Strader LC, Culler AH, Cohen JD, Bartel B (2010) Conversion of endogenous indole-3-butyric acid to indole-3-acetic acid drives cell expansion in Arabidopsis seedlings. *Plant Physiol.* **153**, 1577-1586.
37. Korasick DA, Enders TA, Strader LC (2013) Auxin biosynthesis and storage forms. *J. Exp. Bot.* **64**, 2541-2555.

38. LeClere S, Tellez R, Rampey RA, Matsuda SPT, Bartel B (2002) Characterization of a family of IAA-amino acid conjugate hydrolases from *Arabidopsis*. *J. Biol. Chem.* **277**, 20446-20452.
39. Eyer L, Vain T, Pařízková B, Oklestkova J, Barbez E, Kozubíková H, Pospíšil T, Wierzbicka R, Kleine-Vehn J, Fránek M, Strnad M, Robert S, Novak O (2016) 2,4-D and IAA amino acid conjugates show distinct metabolism in *Arabidopsis*. *PLoS One* **11**, e0159269.
40. McErlich AF, Boydston RA (2013) Current state of weed management in organic and conventional cropping systems. *Publications from USDA-ARS / UNL Faculty Paper* 1387.
41. Steiner HY, Halpin C, Jez JM, Kough J, Parrott W, Underhill L, Weber N, Hannah LC (2013) Evaluating the potential for adverse interactions within genetically engineered breeding stacks. *Plant Physiol.* **161**, 1587-1594.
42. Minor W, Cymborowski M, Otwinowski Z, Chruszcz, M (2006) HKL-3000: the integration of data reduction and structure solution - from diffraction images to an initial model in minutes. *Acta Crystallogr. D* **62**, 859-866.
43. Adams PD, Afonine PV, Bunkóczi G, Chen VB, Davis IW, Echols N, Headd JJ, Hung LW, Kapral GJ, Grosse-Kunstleve RW, McCoy AJ, Moriarty NW, Oeffner R, Read RJ, Richardson DC, Richardson JS, Terwilliger TC, Zwart PH (2010) PHENIX: a comprehensive Python-based system for macromolecular structure solution. *Acta Crystallogr. D* **66**, 213-221.
44. Emsley P, Cowtan K (2004) Coot: model-building tools for molecular graphics. *Acta Crystallogr. D* **60**, 2126-2132.

TABLES

Table 1. Kinetic comparison of Arabidopsis GH3 proteins with auxinic herbicides (2,4-D and 2,4-DB) and auxins (IAA and IBA).

substrate	parameter	AtGH3.1	AtGH3.2	AtGH3.5	AtGH3.15	AtGH3.17
2,4-D	k_{cat} (min^{-1})	--	--	--	1.3 ± 0.1	--
	K_m (μM)	--	--	--	$3,790 \pm 420$	--
	k_{cat}/K_m ($\text{M}^{-1} \text{s}^{-1}$)	--	--	--	6	--
2,4-DB	k_{cat} (min^{-1})	--	11 ± 1.7	3.4 ± 0.4	11 ± 0.7	1.9 ± 0.5
	K_m (μM)	--	$2,330 \pm 260$	$1,160 \pm 190$	590 ± 100	$4,830 \pm 790$
	k_{cat}/K_m ($\text{M}^{-1} \text{s}^{-1}$)	--	78	48	315	6
IAA	k_{cat} (min^{-1})	5.7 ± 0.6	17 ± 1.6	14.5 ± 1.4	0.8 ± 0.1	2.7 ± 0.1
	K_m (μM)	530 ± 150	510 ± 105	770 ± 110	560 ± 160	68 ± 6
	k_{cat}/K_m ($\text{M}^{-1} \text{s}^{-1}$)	179	556	314	23	662
IBA	k_{cat} (min^{-1})	17 ± 20	17 ± 1.8	72 ± 40	9.9 ± 0.2	1.2 ± 0.1
	K_m (μM)	$17,000 \pm 12,500$	$2,190 \pm 390$	$16,500 \pm 9,630$	530 ± 43	$1,600 \pm 160$
	k_{cat}/K_m ($\text{M}^{-1} \text{s}^{-1}$)	17	129	73	313	13

Steady-state kinetic parameters for the auxinic herbicides were determined using varied concentrations of either 2,4-D or 2,4-DB at fixed concentrations of amino acid (10 mM) and ATP (1 mM). The amino acid substrate used for each GH3 protein was follows: AtGH3.1, Asn; AtGH3.2 and AtGH3.5, Asp; AtGH3.15, Gln; and AtGH3.17, Glu. Kinetic parameters for IAA with AtGH3.1, AtGH3.2, AtGH3.5, and AtGH3.17 were previously published (32). Kinetic parameters for IAA and IBA with AtGH3.15 and for IBA with the other proteins were previously published (33). Average values \pm SD (n=3) are shown.

Table 2. Steady-state kinetic analysis of AtGH3.15.

substrate	k_{cat} (min^{-1})	K_m (μM)	k_{cat}/K_m ($\text{M}^{-1} \text{s}^{-1}$)
2,4-DB	11.0 ± 0.7	590 ± 100	315
Gln	52.3 ± 1.5	970 ± 100	887
Cys	52.5 ± 9.7	$7,240 \pm 2,100$	119
His	43.1 ± 1.2	$9,290 \pm 620$	78
Met	27.5 ± 0.6	$10,600 \pm 590$	42
Tyr	12.0 ± 1.8	$18,400 \pm 4,100$	11

Steady-state kinetic parameters were determined using varied concentrations of 2,4-DB at fixed concentrations of Gln (10 mM) and ATP (1 mM) or with varied concentrations of the indicated amino acid at fixed concentrations of 2,4-DB (10 mM) and ATP (1 mM). Average values \pm SD (n=3) are shown. Kinetic parameters for 2,4-DB from Table 1 are shown for comparison.

Table 3. Kinetic analysis of AtGH3.15 with phenoxyalkanoic and phenylalkyl acids.

substrate	k_{cat} (min ⁻¹)	K_m (μM)	k_{cat}/K_m (M ⁻¹ s ⁻¹)
IBA	9.9 ± 0.2	530 ± 40	313
2,4-D	1.3 ± 0.1	3,790 ± 420	6
2,4-DB	11.0 ± 0.7	590 ± 100	315
2,4,5-trichlorophenoxyacetic acid (2,4,5-T)	4.3 ± 0.2	23,200 ± 2,300	3
4-(4-chloro-2-methylphenoxy)butanoic acid (MCPB)	15.6 ± 0.5	1,130 ± 100	228
4-(2-chlorophenoxy)butanoic acid	24 ± 1.4	3,550 ± 520	113
4-(2,6-dimethylphenoxy)butanoic acid	5.4 ± 0.3	180 ± 70	506
4-(4-methoxyphenoxy)butanoic acid	29.8 ± 2.9	14,800 ± 2,470	28
4-phenoxybutyric acid	16.2 ± 3.8	2,140 ± 260	126
4-phenylbutyric acid	15.0 ± 0.5	6,000 ± 420	42
5-phenylvaleric acid	26.6 ± 0.3	960 ± 50	445
5-(4-fluorophenyl)valeric acid	24.0 ± 0.4	680 ± 50	597

Steady-state kinetic parameters were determined using varied concentrations of each substrate with fixed concentrations of Gln (10 mM) and ATP (1 mM). Average values ± SD (n=3) are shown. Kinetic parameters for IBA, 2,4-D, and 2,4-DB from Table 1 are shown for comparison.

Table 4. Summary of crystallographic statistics for the AtGH3.15•2,4-DB complex.Data Collection

Space group	C222 ₁
Cell dimensions	$a = 153.8 \text{ \AA}$, $b = 154.8 \text{ \AA}$, $c = 73.4 \text{ \AA}$
Wavelength (Å)	0.979
Resolution (Å) (highest shell)	38.7 - 2.15 (2.19- 2.15)
Reflections (total/unique)	319,808 / 47,900
Completeness (highest shell)	99.5% (98.1%)
$\langle I/\sigma \rangle$ (highest shell)	18.5 (2.0)
R _{sym} (highest shell)	4.7% (55.7%)

Refinement

R _{cryst} / R _{free}	0.182 / 0.213
No. of protein atoms	4,513
No. of waters	290
No. of ligand atoms	26
R.m.s.d., bond lengths (Å)	0.009
R.m.s.d., bond angles (°)	0.919
Avg. B-factor (Å ²): protein, water, ligand	44.9, 87.0, 48.5
Stereochemistry: most favored, allowed, disallowed	98.4, 1.4, 0.2 %

FIGURE LEGENDS

Figure 1. Structures of phenoxyalkanoic acid auxinic herbicides and endogenous auxins.

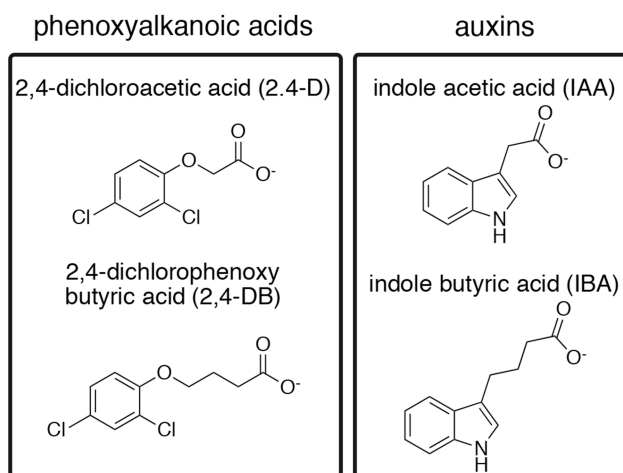


Figure 2. Comparison of Arabidopsis GH3 proteins auxinic herbicide (2,4-D and 2,4-DB) and auxin (IAA and IBA) substrate profiles. Catalytic efficiencies (k_{cat}/K_m) for AtGH3.1, AtGH3.2, AtGH3.5, AtGH3.15, and AtGH3.17 with 2,4-D (black), IAA (grey), 2,4-DB (dark grey), and IBA (white) are summarized based on steady-state data from Table S1.

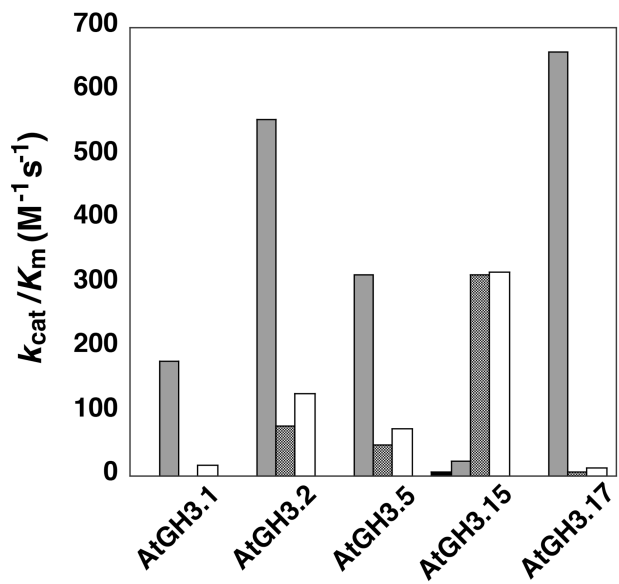


Figure 3. X-ray crystal structure of AtGH3.15 in complex with 2,4-DB. **(A)** Overall three-dimensional structure of the AtGH3.15•2,4-DB complex. The ribbon diagram shows the N- and C-terminal domains with α -helices (rose) and β -strands (blue). The bound 2,4-DB molecules are shown as space-filling models. **(B)** Electron density for 2,4-DB molecules in the active site is shown as a $2F_o-F_c$ omit map (1.0σ). **(C)** Surface view of 2,4-DB binding in the AtGH3.15 active site. The position of AMP from the previously reported AtGH3.15•AMP complex (33) is also shown. **(D)** AtGH3.15 acyl acid binding site. The position of AMP from the previously reported AtGH3.15•AMP complex (33) is also shown.

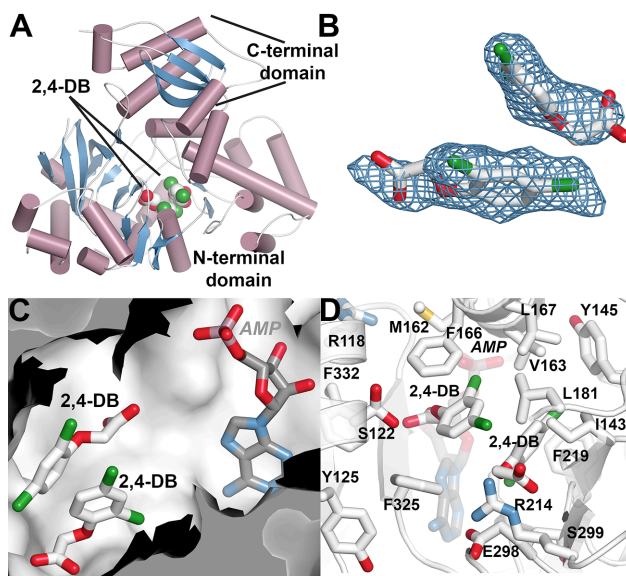


Figure 4. AtGH3.15 knockout and overexpression results in hypersensitivity and resistance to 2,4-DB in root elongation assays. Wild-type Col-0 (Col); Overexpression lines (35S: FLAG-GH3.15) are indicated as GH3.15 1-5, 2-7, and 8-2. **(A)** Seedlings were grown under continuous white light for 10 days at 22 °C on medium supplemented with ethanol (mock) or 1 μ M 2,4-DB. Scale bar = 1 cm. **(B)** Percent root length versus mock-treated was calculated via the equation (root length of treated seedlings)/(average root length of mock treated seedlings)*100. Error bars represent \pm SE of the means (n = 20). * P < 0.05, ** P < 0.001, *** P < 0.0001 versus wild-type.

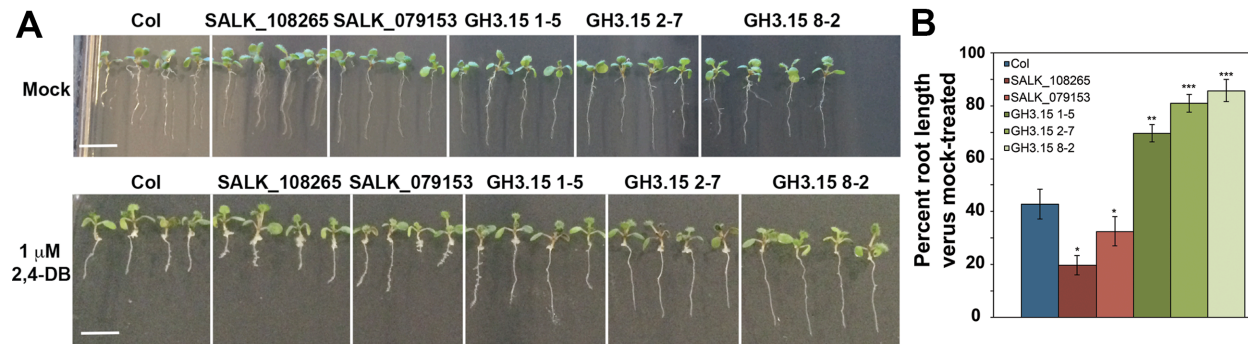
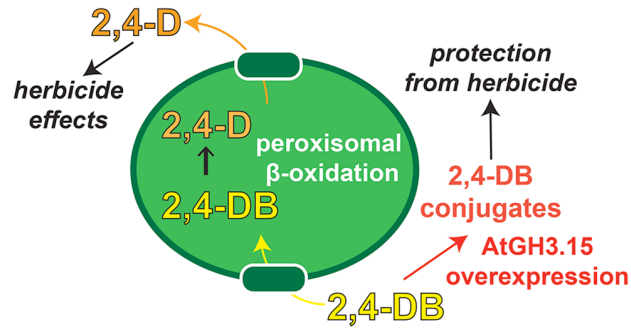


Figure 5. Conversion of 2,4-DB to 2,4-D and potential role of AtGH3.15 as a 2,4-DB tolerance mechanism. Metabolism of 2,4-DB to 2,4-D by β -oxidation in the peroxisome leads to auxinic herbicide effects. Overexpression of AtGH3.15 likely inactivates 2,4-DB by conjugate formation.



Modification of auxinic phenoxyalkanoic acid herbicides by the acyl acid amido synthetase GH3.15 from Arabidopsis

Ashley M. Sherp, Soon Goo Lee, Evelyn Schraft and Joseph M. Jez

J. Biol. Chem. published online October 12, 2018

Access the most updated version of this article at doi: [10.1074/jbc.RA118.004975](https://doi.org/10.1074/jbc.RA118.004975)

Alerts:

- [When this article is cited](#)
- [When a correction for this article is posted](#)

[Click here](#) to choose from all of JBC's e-mail alerts